Low Cost Self-Oscillating ZVS-CV Driver for Power LEDs

E. Mineiro Sá Jr.*, F. L. M. Antunes** and A. J. Perin*
* Federal University of Santa Catarina - UFSC/Electric Engineering Department/INEP, Florianópolis, Brazil
** Federal University of Ceará - UFC/Electric Engineering Department/GPEC, Fortaleza, Brazil
edilson.mineiro@gmail.com, fantunes@dee.ufc.br, arnaldo.perin@inep.ufsc.br

***Abstract*—This paper presents a self-oscillating zero-voltage-switching clamped-voltage (ZVS-CV) power electronics driver for LED strings. A simplified mathematical model of LED has been obtained and used to characterize the series resonant converter for the power LED driver. For a large voltage at the input, this converter does not need a current sensor to stabilize the average current through the LED string. By using the proposed converter the effects of the LED manufacturing tolerances and temperature drifts almost has no influence on the LED string average current, and this is analyzed with the application of the LED electrical model. The simplification of the control design, and of the converter, reduces the component number and the cost. The prototype utilizes a low cost series saturable transformer to drive the bipolar transistors (BJT's). The saturable transformer is a component of the self-oscillating drives and determines the switching frequency of the resonant converter. Analytical results are verified by laboratory experiment.**

I. INTRODUCTION

In the past few years there has been an increased penetration of Solid State Lighting (SSL) into the lighting market, which is mainly caused by the enhanced efficiency, energy savings and flexibility associated to this technology. Nowadays, the SSL has been used in some niche applications as sign boards, traffic lights, automotive head lights and architecture implementations. Some authors estimate that in the near future the SSL will replace standard lamps used in general illumination.

The extended lifetime inherent to the Light Emitting Diode (LED) qualifies SSL to compete with other technologies in the market. In regard to security, SSL has the advantage of being operated at low voltage levels, when compared to other technologies. The electrical shock hazard is reduced when the driver is isolated from the electrical grid [1].

At present, push-pull or half-bridge series-parallel resonant topologies have been employed in electronic ballast for fluorescent lamp. Nevertheless, based on the considerations of cost and reliability, most off-line electronic ballasts adopt self-oscillating half-bridge inverters [2]. These topologies can provide high power density, low switching losses and low EMI contribution. Therefore, these topologies are also of interest for LED applications, because in many cases these topologies operate as current source, which is ideal for the LEDs operation. Up to now few papers have been published concerning resonant operation of LED drivers (e.g. [3] and [4]). Thus, the investigation of a resonant LED driver concept will be carried out in more detail.

This paper presents a self-oscillating zero-voltage-switching clamped-voltage (ZVS-CV) power electronics driver for LED strings. The mathematical model of LED has been obtained and used to characterize the series resonant converter for the power LED driver. Considering the possible of a low cost driver, the prototype utilizes a series saturable transformer to drive the bipolar transistors (BJT's). Depending on the circuit design, the oscillation frequency is usually around tens of kilohertz and can be increased by shortening the BJT storage time. This topology can be implemented with MOSFET devices in a frequency around hundred of kilohertz, but this increase the driver cost. Analytical results are verified by laboratory experiment.

II. LED ELECTRICAL MODEL

The white LED LUXEON III Emitter LXHL-PW09, produced by Philips-Lumileds, was used to implement this driver. Fig. 1 shows an I-V curve for this LED for a temperature of 40°C.

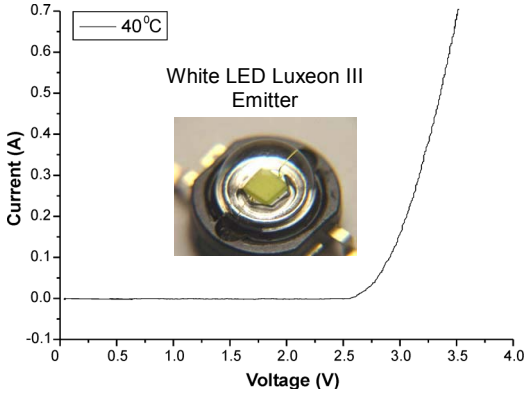

Figure 1. I-V curve of the white LED LUXEON III @40°C.

For high current level the forward voltage, V_F, can be approximated by equation (1). In this equation I_F is the LED current, V_{LED} is the linear coefficient and R_{LED} is the angular coefficient. The R_{LED} represents the series intrinsic resistance in the power LED. The series resistance causes the inclination in the curve and is the main factor responsible for ohmic losses.

$$V_F = V_{LED} + R_{LED} \cdot I_F \quad (1)$$

The LED can be represented by a simplified electrical model as shown in Fig. 2 [5-6]. This electrical model has a good accuracy for current values near the LED rated current.

978-1-4244-1668-4/08/$25.00 ©2008 IEEE

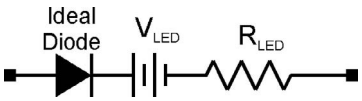

Figure 2. LED simplified electrical model.

Fig. 3 shows that V_{LED} is linearly dependent on the LED junction temperature [6].

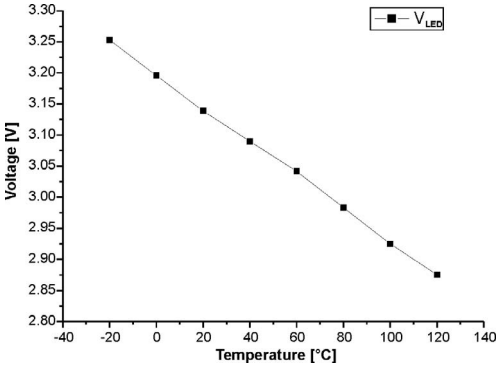

Figure 3. LED junction temperature influence on V_{LED}.

Fig. 4 shows the junction temperature influence on the series resistance. This resistance can usually be considered as constant, because the junction temperature has small influence on the value of the series resistance [6].

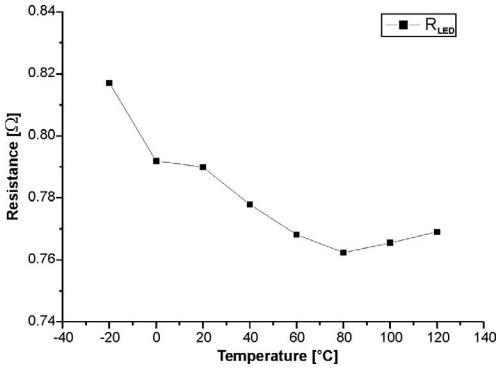

Figure 4. LED junction temperature influence on R_{LED}.

To design the prototype the junction temperature of 60 °C was considered. In this condition V_{LED} is 3.04 V and each LED as R_{LED} equal to 0.77 Ω .

III. Proposed Circuit

Fig. 5 shows the proposed circuit. The ideal diode of the simplified electrical model was incorporated in the output rectifier and the saturable transformer is represented by coils N1, N2 and N3. To obtain the ZVS-CV operation, the series resonant network (LEDs, L_r, C_r and C_{zvs}) should be inductive. To operate with ZVS commutation, the switching frequency of the half-bridge inverter should be higher than the resonant frequency which is the boundary between capacitive and inductive loads. The C_{vzs} capacitance was used to make possible the zero-voltage turn-off operation of the transistors. The startup circuit consists of the RC circuit (Rst and Cst) and a Diac (Dst). The diode Dd is used for continuous discharge of the Cst after startup. The operation stages and saturable transformer design can be obtained in [2], [7] and [8]. Unlike fluorescent or other discharge lamps, LEDs do not require an ignition voltage for the start-up, and the circuit operates always with constant frequency.

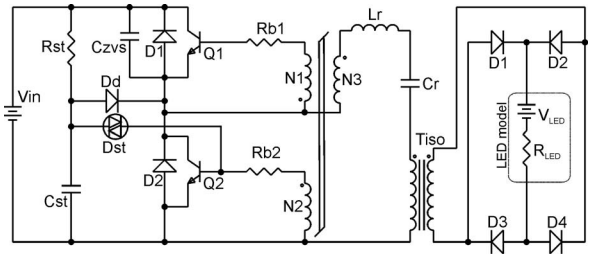

Figure 5. The BJT half-bridge self-oscillating LED driver.

For the sake of simplicity let's assume, in Fig. 5, that the transformer T_{iso} is an isolation transformer, with 1:1 turn ratio, and the core reluctance is infinite. The resistance R_{LED} can be extracted from the bridge rectifier without any change in the final results. In this case, the circuit of Fig. 5 can be simplified to the one presented in Fig. 6, where V_{ab} is a quadratic waveform oscillating between two levels: zero voltage and V_{in}. The voltage V_{LED} can be transformed into an ac square wave, V'_{LED}, in series with R_{LED}, C_r and L_r.

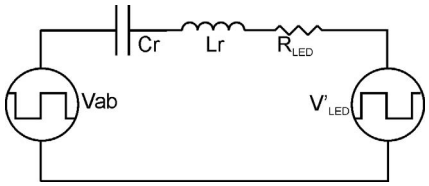

Figure 6. Equivalent circuit.

Considering the first order Fourier, Fig. 6 can be simplified like Fig. 7, where v(t) is defined in equation (2). The voltage source V'_{LED} was transferred to the dc link as a constant dc voltage source V_{LED} which opposes the dc supply V_{in}.

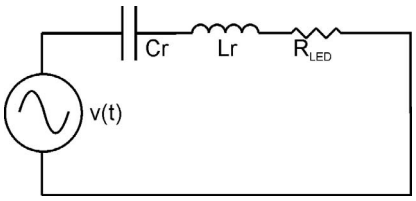

Figure 7. Equivalent circuit.

$$v(t) = \frac{2\left(V_{in} - V_{LED}\right)}{\pi} \cdot \sin\left(\omega \cdot t\right) \tag{2}$$

The RMS value of the voltage v(t) is expressed in equation (3).

$$V_{RMS} = \frac{2\left(V_{in} - V_{LED}\right)}{\pi \cdot \sqrt{2}} \tag{3}$$

The RMS value of the LED current can be expressed in equation (4).

$$I_{RMS} = \frac{V_{RMS}}{\sqrt{R_{LED}^2 + \left(\omega \cdot L_r - \frac{1}{\omega \cdot C_r}\right)^2}} \tag{4}$$

The resonant angular frequency can be defined in equation (5).

$$\omega_o = \frac{1}{\sqrt{L_r \cdot C_r}} \tag{5}$$

Applying (5) in (4) equation (6) can be obtained.

$$I_{RMS} = \frac{V_{RMS}}{\sqrt{R_{LED}^2 + \left(\frac{\omega}{\omega_o^2 \cdot C_r} - \frac{1}{\omega \cdot C_r}\right)^2}} \tag{6}$$

Applying (3) in (6) equation (7) can be obtained.

$$I_{RMS} = \frac{2 \cdot (V_{in} - V_{LED})}{\pi \cdot \sqrt{2} \cdot \sqrt{R_{LED}^2 + \left(\frac{\omega}{\omega_o^2 \cdot C_r} - \frac{1}{\omega \cdot C_r}\right)^2}} \tag{7}$$

The average current through the LED string can be obtained by equation (8) for full wave rectification.

$$I_{AGV} = \frac{I_{RMS} \cdot 2\sqrt{2}}{\pi} \tag{8}$$

Applying (7) in (8) equation (9) can be obtained.

$$I_{AVG} = \frac{4 \cdot (V_{in} - V_{LED})}{\pi^2 \cdot \sqrt{R_{LED}^2 + \left(\frac{\omega}{\omega_o^2 \cdot C_r} - \frac{1}{\omega \cdot C_r}\right)^2}} \tag{9}$$

If $V_{in} \gg V_{LED}$ the equation (9) can be approximated by equation (10). In this case the average current does not depend on the LED voltage and the circuit has a current source characteristics.

$$I_{AVG} \approx \frac{4 \cdot V_{in}}{\pi^2 \cdot \sqrt{R_{LED}^2 + \left(\frac{\omega}{\omega_o^2 \cdot C_r} - \frac{1}{\omega \cdot C_r}\right)^2}} \tag{10}$$

The V_{LED} voltage can be expressed by the voltage at 25°C, $V_{LED\_25\ °C}$, and voltage variation due to temperature variation, is expressed by V_{Temp}. This relation is expressed in equation (11).

$$V_{LED} = V_{LED\_25^\circ C} + \Delta V_{Temp} \tag{11}$$

Applying (11) in (9) equation (12) can be obtained.

$$I_{AVG} = \frac{4 \cdot \left[\left(V_{in} - V_{LED\_25^\circ C}\right) - \Delta V_{Temp}\right]}{\pi^2 \cdot \sqrt{R_{LED}^2 + \left(\frac{\omega}{\omega_o^2 \cdot C_r} - \frac{1}{\omega \cdot C_r}\right)^2}} \tag{12}$$

If relation obtained in equation (13) is preserved, the temperature variation did not change the average current in the LED.

$$V_{in} - V_{LED\_25^\circ C} \gg \Delta V_{Temp} \rightarrow Vin - V_{LED\_25^\circ C} - \Delta V_{Temp} \approx V_{in} - V_{LED\_25^\circ C} \tag{13}$$

The forward voltage decreases with increasing LED die junction temperature. But this cause a little variation in the V_{LED}, in the order of -2 mV/°C for white Luxeon III [9], and practically it does not modify the average current through the LED.

The C_r capacitance can be determined by equation (14). After determinating C_r, the L_r inductance can be obtained by equation (5). In the practical design, the relation between natural angular frequency and angular frequency can be determined by equation (15).

$$C_r = I_{AVG} \cdot \frac{\pi}{2\sqrt{2}} \cdot \left(\frac{\omega}{\omega_o^2} - \frac{1}{\omega}\right) \cdot \sqrt{\frac{1}{\left(\frac{\sqrt{2} \cdot (V_{in} - V_{LED})}{\pi}\right)^2 - R_{LED}^2 \cdot \left(\frac{I_{AVG} \cdot \pi}{2\sqrt{2}}\right)^2}} \tag{14}$$

$$\omega_o = \frac{\omega}{1,3} \tag{15}$$

After resonant circuit parameters Cr and Lr are determined the inductance should be adjusted in order to obtain rated average current through the LED.

IV. Ripple Current Reduction

In many cases the ripple current can exceed the maximum current of the LED. But inserting the capacitor C_f in parallel with the LED the ripple can be reduced. The modified circuit is shown in Fig. 7.

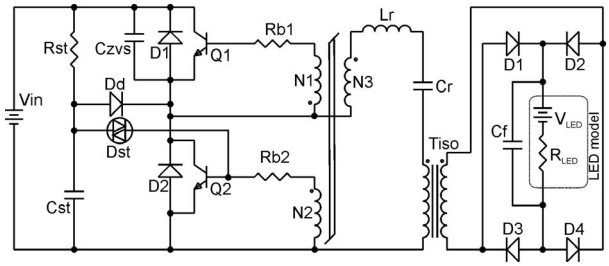

Figure 7. The BJT half-bridge self-oscillating LED driver with output capacitor.

For low current ripple through the LED, the capacitor voltage V_{Cf} can be considered constant. This voltage across C_f can be determined by equation (16).

$$V_{Cf} = V_{LED} + I_{AVG} \cdot R_{LED} \tag{16}$$

Applying the same simplification used before, the simplified circuit can be represented by Fig. 8, where $v_2(t)$ is defined by (17).

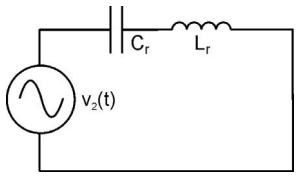

Figure 8. Simplified circuit with C_f capacitor.

$$v_2(t) = \frac{2\left(V_{in} - V_{Cf}\right)}{\pi} \cdot \sin\left(\omega \cdot t\right) \tag{17}$$

The average current in the LED string can be determined by (18).

$$I_{AVG} = \frac{4 \cdot \left(V_{in} - V_{Cf}\right)}{\pi^2 \cdot \left(\frac{\omega}{\omega_o^2 \cdot C_r} - \frac{1}{\omega \cdot C_r}\right)} \tag{18}$$

The resonant capacitor C_r can be determined by (19).

$$C_r = I_{AVG} \cdot \frac{\pi^2 \cdot \left(\frac{\omega}{\omega_o^2} - \frac{1}{\omega} \right)}{4 \cdot \left(V_{in} - V_{Cf} \right)} \tag{19}$$

The resonant inductor Lr can be obtained through the resonant angular frequency defined in equation (5). The inductor can be adjusted through equation (20) for the rated current of the LED.

$$I_{AVG} = \frac{4 \cdot \left(V_{in} - V_{Cf} \right)}{\pi^2 \cdot \left(\omega \cdot L_r - \frac{1}{\omega \cdot C_r} \right)} \tag{20}$$

The output current in the full bridge rectifier can be approximated by a rectified sinusoidal waveform (i_{ret}). This waveform can be decomposed in the Fourier series represented in equation (21).

$$i_{ret}(t) = \sqrt{2} \cdot I_{RMS} \cdot \left[\frac{2}{\pi} - \frac{4}{3\pi} \cos(2\omega t) - \frac{4}{15\pi} \cos(4\omega t) - \ldots \right] \tag{21}$$

For simplification only the fundamental component was used. The RMS value of the fundamental component of the current can be determined by equation (22).

$$I_{F\_RMS} = \frac{4}{3\pi} \cdot I_{RMS} \tag{22}$$

For the fundamental component the simplified circuit shown in Fig. 9 can be used to determine the current ripple through the LED.

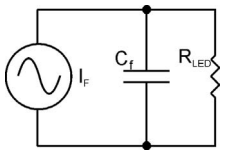

Figure 9. Simplified circuit for determination the value C_f capacitor.

The RMS value of the current through the LED can be determinate by equation (23).

$$I_{LED\_RMS} = \frac{I_{F\_RMS}}{\sqrt{1 + \left(2 \cdot \omega \cdot C_f \cdot R_{LED} \right)^2}} \tag{23}$$

Replacing the RMS current by the average current in equation (23) the equation (24) is obtained.

$$I_{LED\_RMS} = \frac{\frac{\sqrt{2}}{3} \cdot I_{AVG}}{\sqrt{1 + \left(2 \cdot \omega \cdot C_f \cdot R_{LED} \right)^2}} \tag{24}$$

The current ripple can be determinate by equation (25).

$$\Delta I_{LED} = \frac{\frac{4}{3} \cdot I_{AVG}}{\sqrt{1 + \left(2 \cdot \omega \cdot C_f \cdot R_{LED} \right)^2}} \tag{25}$$

The current ripple as a percentage of the average current can be determinate by equation (26).

$$\Delta I_{R_{LED}\_\%} = \frac{\Delta I_{R_{LED}}}{I_{AVG}} = \frac{\frac{4}{3}}{\sqrt{1 + \left(2 \cdot \omega \cdot C_f \cdot R_{LED} \right)^2}} \tag{26}$$

From equation (26) the capacitance C_f can be obtained as stated in equation (27).

$$Cf = \sqrt{\frac{1}{4 \cdot \omega^2 \cdot R_{LED}^2} \cdot \left[\left(\frac{4}{3 \cdot \Delta I_{R_{LED}\_\%}} \right)^2 - 1 \right]} \tag{27}$$

For low ripple current the equation (28) is valid.

$$\left(\frac{4}{3 \cdot \Delta I_{R_{LED}\_\%}} \right)^2 \gg 1 \tag{28}$$

Preserving the relation (28) equation (27) can be simplified as represented in equation (29).

$$Cf \simeq \frac{2}{3 \cdot \Delta I_{R_{LED}\_\%} \cdot \omega \cdot R_{LED}} \tag{29}$$

V. Simulation Results

The simulation in the ORCAD/PSPICE was used to validate the equations and the implemented circuit is shown in Fig. 10. The load is a combination of the eight LEDs in series. For this simulation R_{LED} = R10 = 8 x 0.77 Ω and V_{LED} = V2 = (8 x 3.04 V) – V_{Dbreak}, where V_{Dbreak} is the forward voltage of the diode D12 (1.6 V). The transformer T_{iso} was represented by L1, L2 and K2. The turn ratio used in T_{iso} was 2:1. The load was reflected to the primary of the transformer. For this simulation a 311 V dc link was used. The other circuit parameters are as follows: L_r = L6 = 3.95 mH, C_r = C1 + C2 = 2 x 5.6 nF, C_{zvs} = C3 = 2.7 nF, Rb1 = Rb2 = R4 = R5 = 10 Ω.

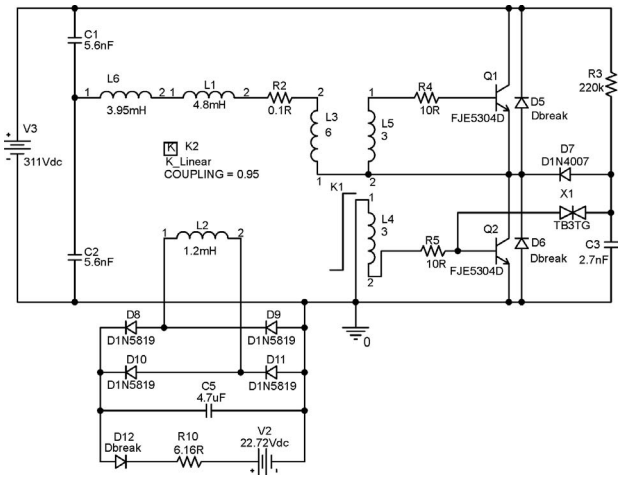

Figure 10. Circuit used for simulation.

The BJT FJE5304D model, bipolar junction transistor produced by Fairchild, was used in Q1 and Q2. The BJT's storage time was 7.4 µs. To determine C_f it was used a ripple of 15% and for this simulation a 4.7 µF capacitor was used.

The saturable transformer was designed to operate with a switching frequency of 28.5 kHz. The saturable core NT-10/5/3,2-1300-TH50, produced by Thornton, was used to implement this transformer. The coil N1 have six

turns, coil N2 have three turns and coil N3 have three turns. The saturable core model K1 used in the simulation is shown in Fig. 11.

```
*DEVICE=NT10_5_3_1300_TH50,CORE
.model NT10_5_3_1300_TH50 CORE (LEVEL=3  OD=1
ID=0.5  AREA=0.077  GAP=0  BR=2500  BM=3900  HC=0.1257)
```

Figure 11. Saturable core model used in ORCAD/PSPICE.

Fig. 12 shows simulation result of the current in the LEDs with low average current crest factor.

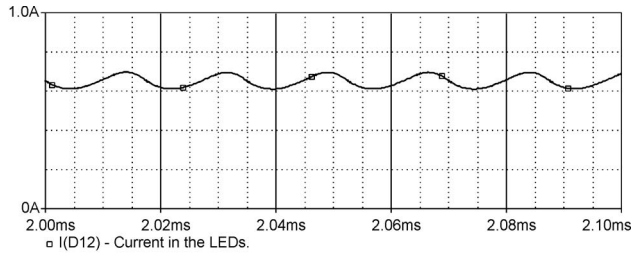

Figure 12. Simulation result of the current in the LED string.

Fig. 13 shows simulation result of the voltage in the saturable transformer (N2).

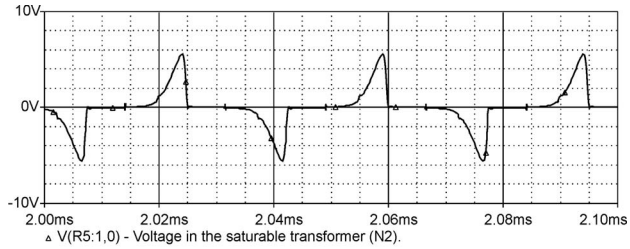

Figure 13. Simulation result of the voltage in N2.

Fig. 14 shows simulation result of the current in the resonant circuit.

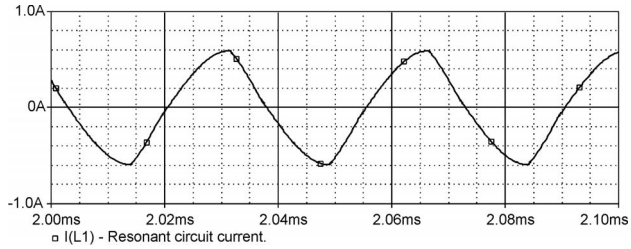

Figure 14. Current in the resonant. circuit.

VI. Experimental Results

The same circuit parameters used for simulation are used in this experiment. For this prototype a 4.7 µF polyester capacitor was used in C_f. The metallic box of the LED driver was used with heatsink to Q1 and Q2.

The load is composed by eight white LEDs Luxeon III Emitter LXHL-PW09. These LEDs are assembled in an aluminum lighting luminary with epoxy painting. The lighting luminary is used with a heatsink and is shown in Fig. 15. To isolate and fix the LED slug a double face thermal conductor adhesive was used (SILGLASS 150 produced by Implastec).

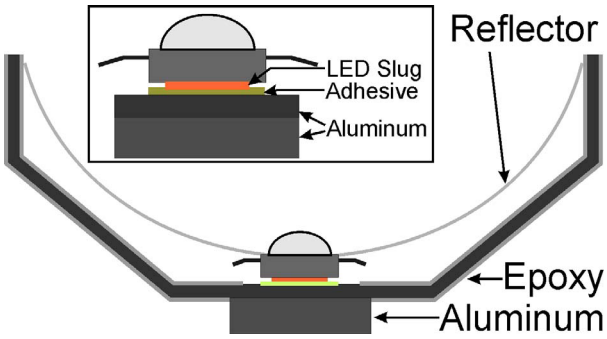

Figure 15. Lighting luminary with a LED assembled.

Fig. 16 shows the resonant circuit current and the voltage in the saturable transformer (turn N2).

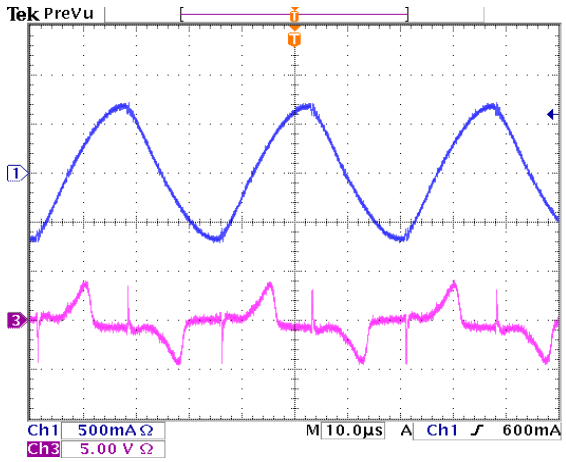

Figure 16. Resonant circuit current and the voltage in the saturable transformer.

Fig. 17 shows the current in the string LEDs with low average current crest factor. The average current in the LED was 650 mA and the ripple factor was measured equal to 15%.

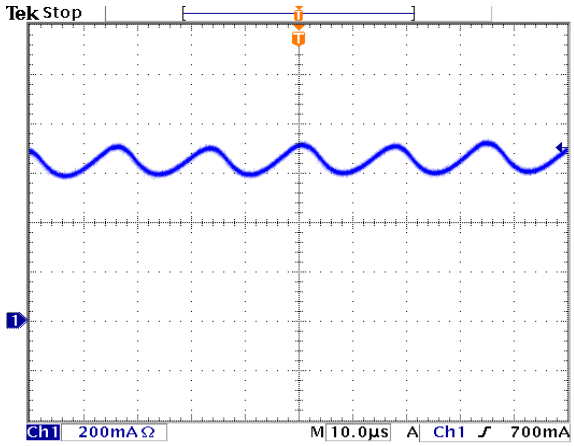

Figure 17. The current in the LED string.

The dc link can be connected to a rectifier output with a filter capacitor which allows the direct connection to the electric grid. Fig. 18 shows current ripple through the LED for a rectifier output filter capacitor of 10 µF. In this case the magnitude of the electric grid was 220 V.

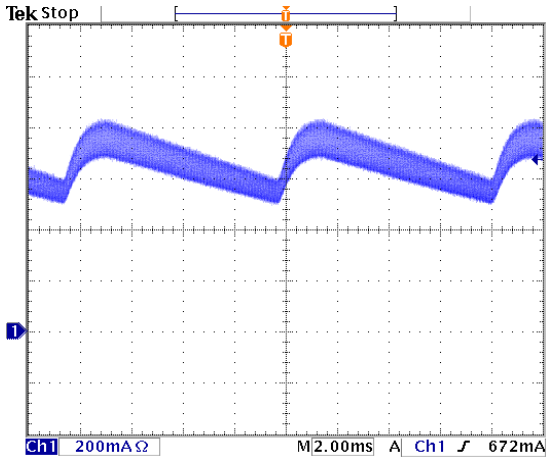

Figure 18. The current in the LED string to a capacitor for filter of 10 µF.

Fig. 19 shows the lighting luminary with eight power LEDs. The LEDs was fixed in the lighting luminary base.

Figure 19. Lighting luminary with eight power LEDs.

Fig. 20 shows the LED driver positioned in the lighting luminary.

Figure 20. LED driver positioning.

Fig. 21 shows the picture of the implemented circuit LED driver.

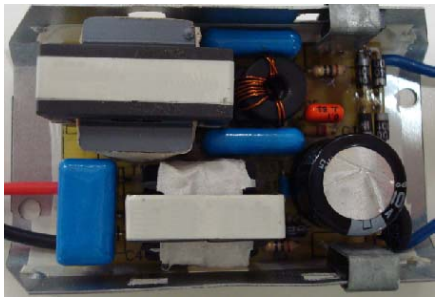

Figure 21. LED driver implemented circuit.

The efficiency of the prototype was equal to 81%, but this can be increased with the use of more efficient magnetic cores.

VII. Conclusions

A low cost self-oscillating ZVS-CV driver for power LEDs was presented. A simplified mathematical model of LED has been obtained and used to characterize the series resonant converter for power LEDs driver. The mathematical analyses were validated through simulation and experimental results.

The LED manufacturing tolerances and drifts over temperature almost has no influence on the LED string average current.

This driver can reduce the costs to replace actual fluorescent lamps for power LEDs.

Like in electronic ballast for discharge lamps, this proposed circuit for power LEDs can be integrated with power factor correction (PFC) structures.

Acknowledgment

The authors acknowledge FINEP, Trancil, Eletrobrás, FUNCAP and CNPq for the financial support to this work.

References

[1] E. Mineiro Sá Jr., E. Agostin Jr., J. Bedin, E. I. Pereira and A. J. Perin "Design of a electronic driver for LEDs", *COBEP 07 - 9º Brazilian Power Electronics Conference,* pp.341-346, 2007.

[2] Y.-R. Yang and C.-L. Chen, "Steady-State Analysis and Simulation of a BJT Self-Oscillating ZVS-CV Ballast Driven by a Saturable Transformer", *IEEE Trans. On Industrial Electronics,* vol. 46, no. 2, pp. 249-260, April 1999.

[3] S. M. Baddela and D. S. Zinger, "Parallel Connected LEDs Operated at High Frequency to Improve Current Sharing*", IEEE Industrial Applications Conference - IAS,* pp. 1677-1681, 2004.

[4] H. van der Broeck, G. Sauerlander and M. Wendt, "Power driver topologies and control schemes for LEDs", *IEEE Applied Power Electronics Conference – APEC*, pp. 1319-1325, 2007.

[5] L. S. Marques, E. Mineiro Sá Jr., F. L. M. Antunes and A. J. Perin, "Step Down Current Controlled dc-dc Converter to Drive a High Power Led Matrix Employed in an Automotive Headlight", *COBEP 05 - 8º Brazilian Power Electronics Conference,* pp.474-478, 2005.

[6] E. Mineiro Sá Jr., F. L. M. Antunes and A. J. Perin, "Junction Temperature Estimation for High Power Light-Emitting Diodes" *IEEE- International Symposium on Industrial Electronics – ISIE,* pp. 3030-3035, 2007.

[7] Y.-R. Yang and C.-L. Chen, "Analysis of self-excited electronic ballast using BJTs/MOSFETs as switching devices", *IEE Proceedings Circuits, Devices and Systems,* vol. 145, Issue 2, pp. 95-104, April 1998.

[8] M. Bairanzade, "Electronic Lamp Ballast Design", *Application Note ON-SEMI AN1543/D,* September 2000.

[9] Philips-Lumileds, "LUXEON III Emitter", *DS-45 Datasheet*, 2006.